

## **DETAILED METHODS**

### ***Sample***

The study involved 277 children from the Chicago area. To be eligible, they had to be in eighth grade (typically 13-14 years old), English-speaking, and in good health, defined as being (a) non-pregnant, (b) without a history of chronic medical or psychiatric illness, (c) free of prescription medications for the past month, (d) without acute infectious disease for two weeks, and (e) without fMRI scanning contra-indications. Each child gave written assent to participate, and a parent or guardian gave written consent. Northwestern University's Institutional Review Board approved the protocol.

The study involved two sessions, typically spaced 1-4 weeks apart. At the first, psychosocial and inflammatory data were collected. Because of venipuncture problems, 2 children were missing inflammation data. At the second session, neural reactivity to threat- and reward-stimuli was measured using fMRI. A number of children did not complete these tasks (32 for threat, 44 for reward) because they did not attend a scanning session, arrived too late to complete the tasks, were too obese or too anxious to enter the scanner, or had previously unrecognized structural anomalies. No useable data was available from another 36 children on the threat task and 59 children on the reward task. The reasons included technical problems with acquisition (brain outside field-of-view), excessive motion (> 10% of TRs censored within a paradigm), or lack of variability in behavioral response. Thus, N for the final analytic sample in threat analyses was 207, and 172 in reward analyses.

Comparisons indicated that children missing fMRI threat-reactivity data were more likely to identify as Black relative to the broader sample ( $p = .003$ ). However, they were similar with regard to

age, sex, Latinx ethnicity, household income, and low-grade inflammation ( $p$ 's from .11 to .80). Similarly, children missing fMRI reward-reactivity data were more likely to identify as Black ( $p = .009$ ), but similar to the broader sample on age, sex, Latinx ethnicity, and household income, ( $p$ 's from .16 to .48). They also displayed more low-grade inflammation relative to the broader sample ( $p = .001$ ), which is unsurprising given that obesity precluded some of them from entering the scanner.

### ***Socioeconomic Conditions***

Children attended the initial session with a parent or guardian, who was interviewed about household finances and composition using the MacArthur Network Sociodemographic Questionnaire (1). To maximize comparability with previous studies of brain development (2, 3), we used household income-to-poverty ratio as the primary indicator of socioeconomic conditions. Parents reported all sources of household income during the previous year, including job wages, government assistance, and workers compensation. They also reported on the number of people living in the household, including dependent children. Using this information, and US government thresholds for 2014, each child's income-to-poverty ratio was computed. To facilitate interpretation of the statistical models, we grouped children into 4 categories, which followed convention in the literature: those in poverty (values  $\leq 0.99$ ), and those whom we refer to as low-income (values of 1.00-1.99), middle-income (values of 2.00-3.99) and higher-income (values  $\geq 4.00$ ) households. In sensitivity analyses, we re-modeled the data treating household income-to-poverty ratio as a continuous variable, and using the MacArthur Scale of Subjective Scale Status (1). This instrument displays a ladder containing 10 rungs, and respondents mark where they stand relative to others in the United States. They are instructed that "At the top of this ladder are the people who are the best off - those who have the most money, the most education, and the most respected jobs. At the bottom are the people who are the worst off-who have the least money, least education, and the least respected jobs or no job."

### ***Low-Grade Inflammation***

Antecubital blood was drawn into a Serum-Separator Tube (Becton-Dickinson), which was centrifuged for 10 minutes at 1200 x g following venipuncture. The serum was harvested and divided into aliquots, then frozen at -80 C until the study ended. We measured serum levels of five inflammatory biomarkers: C-reactive protein (CRP), interleukin-6 (IL-6), interleukin-8 (IL-8), interleukin-10 (IL-10), and tumor necrosis factor- $\alpha$  (TNF- $\alpha$ ). CRP was measured in duplicate with a high-sensitivity immunoturbidimetric assay on a Roche/Hitachi cobas c502 analyzer. The average intra- and inter-assay coefficients of variation were 2.5% and 5.6%, respectively. This assay's lower limit of detection is 0.2 mg/L. The cytokines were measured in triplicate using a multi-plex immunoassay on an automated microfluidic platform (Simple Plex, Protein Simple) (4). Lower limits of detection range from 0.08 pg/mL (IL-8) to 0.28 pg/mL (TNF- $\alpha$ ). Across runs, the average intra-assay coefficients of variation for triplicate samples were 5.05% (IL-6), 2.03% (IL-8), 3.46% (IL-10), and 3.96% (TNF- $\alpha$ ).

Most of the inflammatory biomarkers were skewed and/or kurtotic, but their distributions were normalized after log-10 transformation. Following previous research (5), we standardized the logged values of each biomarker (mean = 0; SD = 1), and averaged the resulting Z-scores to form a composite (Cronbach's alpha = .63) where higher scores reflect more low-grade inflammation. (Readers may wonder about including IL-10 in the composite, since its functions are principally anti-inflammatory. However, IL-10 is only expressed under pro-inflammatory conditions, so empirically it correlates positively with the other biomarkers assessed here.) The composite approach has two advantages. Statistically, it reduces the number of tests performed - here, by 80% - and thus the rate of false-positive results. Biologically, a composite better reflects in vivo conditions, where pro-inflammatory cytokines are released in cascading fashion, and have redundant and synergistic effects on target cells.

### ***Threat Paradigm***

The threat paradigm was a modified version of the morphed faces task (6). (An earlier report examined responses to this task as a function of violence exposure and family income, using a different analytic strategy (7)). Children saw a facial expression displayed for 2000 ms, followed by a blank screen for 1000 ms and a jittered inter-stimulus interval of 500-2500 ms. They were required to indicate, via button press, the gender of the face. The stimuli consisted of still photos of four male and four female actors drawn from a widely used stimulus set (8). For each actor, five angry and five happy images were shown at varying intensity levels (20%, 40%, 60%, 80% and 100% of prototypical). Each image was displayed once in pseudo-random order. Eight trials were presented at each intensity level (for 80 trials total) in a single run lasting 7 minutes and 21 seconds. Given the NIN framework's explicit predictions about threat, we focused here on children's responses to angry expressions relative to fixation. Responses to angry faces were defined as the average of 60%, 80% and 100% of prototypical. Neutral faces, defined as 20% of prototypical for angry and happy expressions, were also modeled and included in the specificity analysis. All other expressions (40% prototypical for angry; 40 to 100% of prototypical for happy) were modeled together as a regressor of no-interest.

### ***Reward Paradigm***

To assess reward processing, children performed a modified version of a passive avoidance task (9), where the goal is to learn which objects result in monetary rewards, and respond accordingly. Each trial involved a 1500 ms presentation of a shape, followed by a randomly jittered fixation period of 500-2500 ms, 1500 ms of feedback, and another randomly jittered fixation period of 0-4000 ms. After each shape was presented, children could respond with a button press, triggering a win or loss event, or ignore the stimulus, triggering a blank screen with no monetary outcome. In trials where children responded, one of four outcomes occurred: win \$50, win \$10, lose \$10 or lose \$50. The feedback was probabilistic and pseudorandom, such that responding to two particular shapes earned money on 87.5%

of trials and responding to the other two shapes lost money 87.5% of trials. In total, children completed 96 trials (24 trials of 4 colored shapes) in one 9 minute and 55 second run. Afterwards, they were paid \$5, regardless of performance.

### **MRI Parameters and Preprocessing**

Scanning took place at the Center for Translational Imaging at Northwestern University. A Siemens Prisma 3 Tesla scanner with a 64 phased-array head/neck coil was used. A T2\* weighted gradient echo planar imaging (EPI) sequence (repetition time=2000 ms; echo time=27 ms; 240 mm field of view; 94x94 matrix; 90° flip angle) was utilized, collecting 202 total images for the threat paradigm and 300 images for the reward paradigm. Whole-brain coverage was obtained with 43 axial slices (voxel size 1.694x1.694x1.7 mm<sup>3</sup>) for both paradigms. Structural imaging consisted of a high-resolution navigated multiecho magnetization prepared rapid acquisition gradient echo sequence (MPRAGE, TR = 2300 ms, TE = 1.86, 3.78; flip angle = 7°; FOV = 256 × 256; matrix = 320 × 320; 208 slices; voxel size = 0.8 mm<sup>3</sup>).

fMRI data were analyzed using Analysis of Functional Neuroimages (AFNI) (10). Functional images were despiked and slice-time and motion corrected. Anatomical scans were registered to the base volume of each child's functional images and warped to standard space (11). Each volume of functional data was then aligned to this base volume and also warped to standard space. All volumes were resampled to 2mm<sup>3</sup>. Functional images were spatially smoothed with a 6mm full-width-half-maximum Gaussian kernel. The time series were then normalized by dividing the signal intensity of a voxel at each time-point by the mean signal intensity of that voxel for each run and multiplying the result by 100. The resultant regression coefficients represent a percentage of signal change from the mean. Because not all children completed both paradigms, this process was performed separately for each EPI sequence.

### ***Individual Level Analysis***

Models for both paradigms included the six motion from preprocessing (see above) and task regressors. For the threat paradigm, task specific regressors were included for angry faces, neutral faces and faces of no-interest. For the reward paradigm, the following task regressors were included: i) cue-phase trials when participants responded to an object, ii) cue-phase trials when participants did *not* respond to an object, iii) rewarding feedback-phase trials, and iv) punishing feedback-phase trials. All regressors were convolved with a canonical hemodynamic response function. Linear regression was performed separately for each paradigm using models including motion and task regressors, as well as a task-specific baseline drift function to correct for slow movement during the scan. Volumes showing  $\geq .5\text{mm}$  movement from the previous volume were censored. This produced  $\beta$  coefficients and associated  $t$  statistics for each voxel and regressor. BOLD response data were extracted for each subject from anatomically defined masks, including an amygdala mask for the threat task (Eickhoff-Zilles Architectonic Atlas: 50% probability mask) (12) and a ventral striatum mask for the reward task (Accumbens-area map) (13). Threat response were operationalized as amygdala response to angry faces (relative to fixation). Amygdala response to neutral faces (relative to fixation) was used in specificity analyses. Reward response was operationalized as ventral striatum response to rewarding feedback-phase trials (relative to fixation). Ventral striatum response (relative to fixation) to punishing feedback-phase trials was used in specificity analyses.

### ***Covariates***

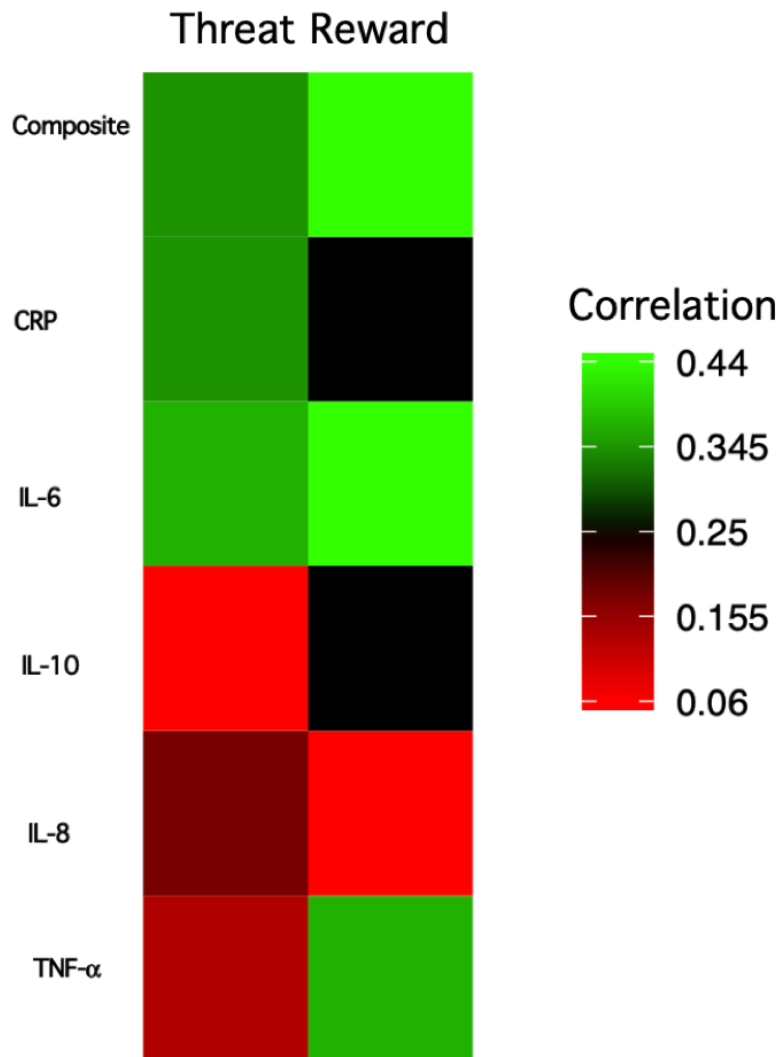
Statistical models included a panel of covariates, chosen a priori, because of their relationship with socioeconomic conditions and/or brain development. They included the child's self-reported age (in years and months), dummy-coded variables reflecting sex (female = 0, male = 1), self-identified racial (non-White = 0; White = 1) and ethnic (non-Latinx = 0; Latinx = 1) category, and pubertal status. The latter was measured with the Peterson Pubertal Development Scale (14), an extensively validated

questionnaire with items that capture sex-specific indicators of maturity, e.g., body hair and voice deepening for males, and the growth of breasts and menstruation for females. Scores on this scale range from 1 (pre-pubertal) to 5 (post-pubertal).

### ***Statistical Approach***

To evaluate study hypotheses, we estimated a series of linear regression equations, using Model 1 of the PROCESS v3.4 routine in SPSS Version 25 (15). The outcome variable was the inflammation composite. Predictors included (a) the covariate panel, (b) a multi-categorical variable reflecting household income-to-poverty ratio, (c) a mean-centered variable reflecting amygdala response to angry faces or striatal response to monetary reward, and (d) a product term representing the interaction between income-to-poverty ratio and amygdala or striatal reactivity. To decipher interactions, we plotted estimated inflammation scores at lower (-1 SD) and higher values (+1 SD) of the relevant neural reactivity distributions. Separate plots were generated for children in each of the four categories of household income-to-poverty ratio. All reported p values are based on two-tailed tests.

**FIGURE S1.** Heatmap depicting the strength of associations between specific inflammatory biomarkers and neural responsiveness to threat and reward stimuli. The correlations are in r units, and have been adjusted for age, sex, race, ethnicity, and poverty status. They are computed for the children living in poverty, who showed consistent associations between the inflammatory composite and neural responsiveness, whereas participants in other socioeconomic conditions did not.





## REFERENCES

1. Adler NE, Epel ES, Castellazzo G, Ickovics JR: Relationship of subjective and objective social status with psychological and physiological functioning: preliminary data in healthy white women. *Health Psychology* 2000;19:586–592
2. Noble KG, Houston SM, Brito NH, Bartsch H, Kan E, Kuperman JM, Akshoomoff N, Amaral DG, Bloss CS, Libiger O, Schork NJ, Murray SS, Casey BJ, Chang L, Ernst TM, Frazier JA, Gruen JR, Kennedy DN, Van Zijl P, Mostofsky S, Kaufmann WE, Kenet T, Dale AM, Jernigan TL, Sowell ER: Family income, parental education and brain structure in children and adolescents. *Nat Neurosci* 2015;18:773–778
3. Luby J, Belden A, Botteron K, Marrus N, Harms MP, Babb C, Nishino T, Barch D: The effects of poverty on childhood brain development: the mediating effect of caregiving and stressful life events. *JAMA Pediatr* 2013;167:1135–1142
4. Aldo P, Marusov G, Svancara D, David J, Mor G: Simple Plex™: A novel multi-analyte, automated microfluidic immunoassay platform for the detection of human and mouse cytokines and chemokines. *Am J Reprod Immunol* 2016;75:678–693
5. Miller GE, Brody GH, Yu T, Chen E: A family-oriented psychosocial intervention reduces inflammation in low-SES African American youth. *Proc Natl Acad Sci U S A* 2014;111:11287–11292
6. Marsh AA, Finger EC, Mitchell DG, Reid ME, Sims C, Kosson DS, Towbin KE, Leibenluft E, Pine DS, Blair RJ: Reduced amygdala response to fearful expressions in children and adolescents with callous-unemotional traits and disruptive behavior disorders. *Am J Psychiatry* 2008;165:712–720

7. White SF, Voss JL, Chiang JJ, Wang L, McLaughlin KA, Miller GE: Exposure to violence and low family income are associated with heightened amygdala responsiveness to threat among adolescents. *Dev Cogn Neurosci* 2019;40:100709
8. Ekman P, Friesen WV: *Pictures of facial affect*, New York, Consulting Psychologists Press, 1976
9. White SF, Geraci M, Lewis E, Leshin J, Teng C, Averbeck B, Meffert H, Ernst M, Blair JR, Grillon C, Blair KS: Prediction error representation in individuals with generalized anxiety disorder during passive avoidance. *Am J Psychiatry* 2017;174:110–117
10. Cox RW: AFNI: software for analysis and visualization of functional magnetic resonance neuroimages. *Comput Biomed Res* 1996;29:162–173
11. Talairach JT, P.: *Co-planar stereotaxic atlas of the human brain: 3D proportional system: An approach to cerebral imaging*, New York, Thieme, 1988
12. Amunts K, Kedo O, Kindler M, Pieperhoff P, Mohlberg H, Shah NJ, Habel U, Schneider F, Zilles K: Cytoarchitectonic mapping of the human amygdala, hippocampal region and entorhinal cortex: intersubject variability and probability maps. *Anat Embryol (Berl)* 2005;210:343–352
13. Destrieux C, Fischl B, Dale A, Halgren E: Automatic parcellation of human cortical gyri and sulci using standard anatomical nomenclature. *Neuroimage* 2010;53:1–15
14. Peterson A, Crockett L, Richards M, Boxer A: A self-report measure of pubertal status: Reliability, validity, and initial norms. *Journal of Youth and Adolescence* 1988;17:117–133
15. Hayes AF: *Introduction to mediation, moderation, and conditional process analysis*, Second Edition, New York, The Guilford Press, 2018